Ultrastructural Changes Associated With Dexamethasone-Induced Ocular Hypertension in Mice

Darryl R. Overby,[1] Jacques Bertrand,[1] Ozan-Yüksel Tektas,*[,2] Alexandra Boussommier-Calleja,[1] Martin Schicht,[2] C. Ross Ethier,[1,3] David F. Woodward,[4] W. Daniel Stamer,[5] and Elke Lütjen-Drecoll[2]

[1]Department of Bioengineering, Imperial College London, London, United Kingdom
[2]Department of Anatomy II, University of Erlangen-Nürnberg, Erlangen, Germany
[3]Department of Biomedical Engineering, Georgia Institute of Technology, Atlanta, Georgia, United States
[4]Department of Biological Sciences, Allergan, Inc., Irvine, California, United States
[5]Department of Ophthalmology, Duke University Medical Center, Durham, North Carolina, United States

Correspondence: Darryl R. Overby, Department of Bioengineering, Imperial College London, London SW7 2AZ, UK; d.overby@imperial.ac.uk.

Current affiliation: *Department of Psychiatry, Friedrick-Alexander University of Erlangen, Erlangen, Germany.

Submitted: March 23, 2014
Accepted: June 29, 2014

Citation: Overby DR, Bertrand J, Tektas O-Y, et al. Ultrastructural changes associated with dexamethasone-induced ocular hypertension in mice. *Invest Ophthalmol Vis Sci*. 2014;55:4922–4933. DOI:10.1167/iovs.14-14429

Purpose. To determine whether dexamethasone (DEX)-induced ocular hypertension (OHT) in mice mimics the hallmarks of steroid-induced glaucoma (SIG) in humans, including reduced conventional outflow facility (*C*), increased extracellular matrix (ECM), and myofibroblasts within the outflow pathway.

Methods. Osmotic mini-pumps were implanted subcutaneously into C57BL/6J mice for systemic delivery of DEX (3–4 mg/kg/d, $n = 31$ mice) or vehicle ($n = 28$). IOP was measured weekly by rebound tonometry. After 3 to 4 weeks, mice were euthanized and eyes enucleated for ex vivo perfusion to measure *C*, for electron microscopy to examine the trabecular meshwork (TM) and Schlemm's canal (SC), or for immunohistochemistry to examine type IV collagen and α-smooth muscle actin. The length of basement membrane material (BMM) was measured along the anterior-posterior extent of SC by electron microscopy. Ultrastructural changes in BMM of DEX-treated mice were compared against archived human SIG specimens.

Results. Dexamethasone increased IOP by 2.6 ± 1.6 mm Hg (mean ± SD) over 3 to 4 weeks and decreased *C* by 52% ± 17% versus controls. Intraocular pressure elevation correlated with decreased *C*. Dexamethasone treatment led to increased fibrillar material in the TM, plaque-like sheath material surrounding elastic fibers, and myofibroblasts along SC outer wall. The length of BMM underlying SC was significantly increased in mice with DEX and in humans with SIG, and in mice decreased *C* correlated with increased BMM.

Conclusions. Dexamethasone-induced OHT in mice mimics hallmarks of human SIG within 4 weeks of DEX treatment. The correlation between reduced *C* and newly formed ECM motivates further study using DEX-treated mice to investigate the pathogenesis of conventional outflow obstruction in glaucoma.

Keywords: steroid glaucoma, trabecular meshwork, basement membrane

In susceptible individuals, sustained corticosteroid therapy causes ocular hypertension (OHT), developing to steroid-induced glaucoma (SIG) and eventual vision loss if not discontinued.[1] Ocular hypertension induced by corticosteroids mimics aspects of primary open-angle glaucoma (POAG) in that both conditions present with open chamber angles and decreased conventional outflow facility[2–4]; furthermore, most patients with POAG experience elevated IOP when treated with corticosteroids.[5,6] Common mechanisms may therefore underlie the pathogenesis of POAG and SIG, motivating further investigation of corticosteroid-induced OHT as an inducible model of conventional outflow dysfunction that may improve our understanding of POAG.[7]

Despite many laboratory studies of corticosteroid-induced OHT in cows,[8–10] cats,[11,12] rabbits,[13] sheep,[14–16] rats,[17] mice,[18–21] monkeys,[22] and humans,[23–26] relatively few studies[9,23,27,28] have examined the morphological basis for corticosteroid-induced outflow obstruction within the trabecular meshwork (TM). In human eyes treated with corticosteroids, fine fibrillar material was observed in the juxtacanalicular connective tissue (JCT) underlying the inner wall of Schlemm's canal (SC),[28] and "fingerprint" like basement membrane material (BMM) was observed in the TM.[23,27] Sheath-derived "plaques" similar to those seen in human eyes with POAG[9] were observed in bovine eyes with corticosteroid-induced OHT. These studies[9,23,27,28] suggest that extracellular matrix (ECM) alterations contribute to conventional outflow obstruction within the TM or JCT, but no studies have yet correlated corticosteroid-induced changes in ECM to outflow facility so as to more precisely identify the ultrastructural basis of corticosteroid-induced OHT.

The trabecular outflow pathway of mice is structurally and functionally similar to that of primates. Like primates, mice have a continuous SC and a lamellated TM,[29] and mice have an elastic fiber net in the TM that tethers the ciliary muscle to the inner wall of SC.[30] Mice exhibit a similar IOP[31] and aqueous humor turnover time[32] to humans and, like human eyes, mouse eyes do not appear to exhibit "wash-out."[33] The pharmacology

of outflow facility regulation in mice also mimics that occurring in humans, with a similar facility response to G-protein–coupled receptor agonists[34] and pilocarpine.[30,35] On account of these similarities, mice provide an appropriate model to study TM function and IOP regulation as relevant for the pathogenesis of human glaucoma. Recently, Whitlock et al.[18] and Zode et al.[21] developed mouse models of glucocorticoid-induced OHT in response to systemic dexamethasone (DEX) and topical ocular DEX, respectively, and Kumar et al.[19,20] showed that triamcinolone acetonide delivered subconjunctivally decreases outflow facility in living mice. The goal of the current study was to determine whether DEX-induced OHT in mice coincides with decreased conventional outflow facility, and whether changes in outflow facility correlate with accumulation of ECM in the JCT, thought to be an important locus of outflow resistance generation.

Methods

Experimental Design

All procedures on living mice were done in compliance with the ARVO Statement for the Use of Animals in Ophthalmic and Vision Research under UK Home Office Project License 70/7306.

Steroid OHT was induced by systemic delivery of DEX over 3 to 4 weeks via a subcutaneous osmotic mini-pump implanted into the lateral back of C57BL/6J mice (Jackson Laboratories, supplied through Charles River Ltd., Margate, UK), following the procedure outlined by Whitlock et al.[18] Intraocular pressure was measured weekly by rebound tonometry. At the end of the 3- to 4-week period, mice were euthanized and their eyes were enucleated for ex vivo perfusion to measure conventional outflow facility. Typically one eye was used for perfusion, while the contralateral eye was prepared for electron microscopy or immunohistochemistry to examine the morphology of the conventional outflow pathway. Results obtained from DEX-treated mice were compared against results from sham-treated control mice that were implanted with osmotic mini-pumps containing vehicle without DEX.

This study used 59 C57BL/6J mice (Jackson Laboratories, Bar Harbour, ME, USA) between 10 and 14 weeks of age at the time of surgery, including 31 DEX-treated and 28 sham-treated control mice separated into three cohorts (19 or 20 per cohort). All mice were male. The osmotic mini-pumps (Alzet, model 1004; DURECT Corp., Cupertino, CA, USA) each hold a volume of 100 μL with a nominal delivery rate of 0.11 μL/h, and the DEX concentration loaded into the mini-pumps was adjusted (30–40 mg/mL) depending on the average body mass of that cohort to achieve a nominal systemic dosage between 3 and 4 mg/kg/d to match the dosage used by Whitlock et al.[18] The DEX was water-soluble (D2915; Sigma-Aldrich Corp., St. Louis, MO, USA), contained cyclodextrin (1.36 g per 100 mg DEX), and was solubilized in PBS. Cyclodextrin was included in the sham-treated control group of cohort 3, but not in controls for cohorts 1 and 2. All solutions were first sterile-filtered through a 0.22-μm inline syringe filter, and the mini-pump reservoirs were filled and prepared within a Class 2 laminar flow bio-safety cabinet and stored in individual sterile tubes.

Animal Husbandry and Surgery

The mice were housed in individually ventilated cages with a 12-hour light/12-hour dark cycle. All mice had access to food and water ad libitum. Following arrival from the commercial supplier, mice were allowed to acclimatize for at least 1 week before surgery. Surgery was performed under general anesthesia induced by 5-minute exposure to 3% to 4% isoflurane and 1.0 to 1.5 L/min oxygen in an anesthetic chamber. Following loss of consciousness, the mouse was transferred to a Bain coaxial circuit (Able Scientific, Perth, Australia) with 3% to 4% isoflurane and 1 L/min oxygen. The surgical site was shaved and sanitized with chlorhexidine alcohol (Krusse, Langeskov, Denmark). The mice were subcutaneously injected near the surgical site with 5 mg/kg carprofen nonsteroidal analgesic (Rimadyl; Pfizer, New York, NY, USA) and 5 mg/kg enrofloxacin antimicrobial (Baytril; Bayer Healthcare, Leverkusen, Germany). In cohort 3, carprofen was replaced by 0.05 mg/kg intramuscular buprenorphine (Vetergesic; Reckitt Benckiser Healthcare, Hull, UK).

A dorsal incision approximately 1 cm long was made along the midline from the base of the scapula, and a subcutaneous pocket was created along the side of the animal using blunt dissection with sterilized surgical scissors. The pump was gently inserted into the pocket with the flow moderator directed posteriorly away from the incision. The pocket was deepened until the wound could be closed completely with the implant in place. Surgical tissue adhesive (Tissue Bond; 3M, St. Paul, MN, USA) was then used to seal the wound margins. Mice were removed from the Bain coaxial circuit and placed in a warm 36°C chamber for recovery. Mice were housed singly and closely monitored for the remainder of the study. Mice that lost significant weight (1–5 g, typical for DEX-treated mice) were given access to a high-caloric dietary supplement (Complan; H. J. Heinz Co., Ltd., Middlesex, UK) or were treated following recommendations by the staff veterinarian. Mice that lost more than 20% of initial body mass were dropped from the study. A second dose of analgesic (carprofen or buprenorphine, as described above) was delivered approximately 12 hours after surgery.

Measurement of Serum DEX Concentration

Serum DEX concentration was measured by high-performance liquid chromatography and tandem mass spectrometry (LC/MS-MS). Whole-blood samples were taken from the tail vein of living mice (20 μL) or from the retro-orbital sinus soon after death (100 μL). Serum was separated from whole blood via centrifugation (12,000*g* for 5 minutes) in Microvettes (Model 100Z; Sarstedt, Nümbrecht, Germany) containing clotting activator. Serum samples were stored at −20°C and shipped overnight on dry ice to a commercial LC/MS-MS service provider (Intertek Pharmaceutical Services, San Francisco, CA, USA) for analysis. Samples were analyzed from 11 DEX-treated and 8 control mice from cohort 2, with samples taken at 3, 10, and 28 days after mini-pump implantation. The service provider performed the calibration using known concentrations of DEX in mouse serum between 2 and 200 ng/mL. The lower limit of quantification was 10 ng/mL for 20-μL samples (days 3 and 10) and 2 ng/mL for 100-μL samples (day 28).

Measurement of IOP

Based on a pilot study that had shown that IOP elevation in response to DEX was similar between left and right eyes, IOP was measured in the right eye of each mouse between 8:00 AM and 12:00 noon by using a commercial rebound tonometer (TonoLab; Icare, Helsinki, Finland) with the mouse under general isoflurane anesthesia. For cohorts 1 and 2, baseline IOP was measured immediately before surgery, and IOP was measured at weekly intervals (typically 7 ± 1 day) for 4 weeks after surgery. For cohort 3, baseline IOP was measured 5 to 8 days before surgery, and IOP was measured at weekly intervals for 3 weeks after surgery. Each IOP measurement was defined as the average of three consecutive tonometer readings taken

Investigative Ophthalmology & Visual Science

directly from the instrument display panel, with each tonometer reading based on six consecutive rebound events, following manufacturer's instructions. The tonometer-reported IOP was then corrected by the calibration curve described below. Occasionally, IOP was measured twice within a weekly interval, and for these cases the average between the two IOP measurements was used for data analysis. For IOP measurements, mice were anesthetized by 2-minute exposure to 3% to 4% isoflurane and 1.0 to 1.5 L/min oxygen in an anesthetic chamber. Mice were then placed in a soft clay mold supported on an adjustable laboratory jack stand using a Bain coaxial circuit to maintain anesthesia with 4% isoflurane. For cohort 1, the tonometer was held by hand during the measurement. For cohorts 2 and 3, the tonometer was mounted on a micromanipulator supported by a ring stand with the tip positioned approximately 2 mm from the central cornea along the optical axis. Attempts to measure IOP on nonanesthetized mice were prevented by difficulties restraining and calming the mice with the implant in place. Because anesthesia decreases IOP in mice,[36–39] the tonometer will likely underestimate the true IOP by 1 to 2 mm Hg, but we did not correct for this effect in any of the cohorts.

The tonometer was calibrated using cadaveric eyes, with IOP controlled manometrically using an adjustable-height reservoir to give a pressure between 8 and 30 mm Hg. Calibration was performed using two eyes from a single DEX-treated mouse and one eye from a single sham-treated mouse, both from cohort 3. The eyes were maintained in situ without enucleation, and the eyes were connected to the reservoir through a 33-G intracameral needle placed near the limbus. The calibration trend line describing the relationship between tonometric and manometric IOP was indistinguishable between DEX- and sham-treated control mice ($P = 0.76$, linear regression, SPSS [IBM, Armonk, NY, USA]; Supplementary Fig. S1). Calibration data from DEX- and sham-treated mice were therefore lumped together to produce a single regression that was used to correct all tonometer measurements (IOP_t) in this study according to

$$IOP = 1.2\,IOP_t - 1.7\,mm\,Hg. \quad (1)$$

Measurement of Conventional Outflow Facility

Typically, one eye (OD) of each mouse was used for ex vivo ocular perfusion to measure conventional outflow facility, while the contralateral (OS) eye was immersion fixed and used for ultrastructural or immunohistochemical analysis (see below). Mice from cohort 1 were euthanized by cervical dislocation; however, this led to an immediate loss of tension and partial collapse of the globe that we attributed to a sudden decrease in episcleral venous pressure following rupture of the cervical vessels. To avoid this effect, mice from cohorts 2 and 3 were euthanized by intraperitoneal pentobarbital (~5 mg). Eyes were enucleated immediately after death and placed in Dulbecco's modified Eagle's medium at room temperature to await perfusion, typically within 30 minutes.

Ex vivo perfusion of enucleated mouse eyes followed previously described techniques.[33,34,39,40] Briefly, eyes were mounted on a plastic post using cyanoacrylate glue and were cannulated by a 33-G needle with the tip positioned in the anterior chamber. The intracameral needle was connected to a pressure transducer (142PC01; Honeywell, Morristown, NJ, USA), and a syringe pump (PHD ULTRA; Harvard Apparatus, Holliston, MA, USA) under the control of a computer programmed[41] using LabVIEW (National Instruments, Austin, TX, USA). Each eye was perfused at successive pressure steps of 4, 8, 15, and 25 mm Hg, with at least 10 minutes of stable perfusion tracing at each pressure step. The average stable flow rate at each step was plotted versus perfusion pressure, and linear regression analysis was used to calculate the slope of the flow versus pressure relationship that represents the conventional outflow facility for that eye.[33] Eyes that achieved stable flow rate tracings for at least three pressure steps were included in the statistical analysis, giving 31 valid perfusions of 45 total attempts. The perfusion solution was Dulbecco's PBS (Life Technologies Ltd., Paisley, UK) with divalent cations and 5.5 mM glucose (referred to as "DBG") that was sterile filtered (0.22 μm) before perfusion. For cohort 1, the eye was perfused at room temperature and covered with tissue paper that was kept moist by regular drops of isotonic saline. For cohorts 2 and 3, the eye was submerged to the limbus in a heated bath (35°C) of isotonic saline with the cornea covered with moist tissue paper. Although we present perfusion data from cohort 1, we focus mainly on data from cohorts 2 and 3 because these were perfused under more physiologic conditions.

Immunohistochemistry and Ultrastructural Analysis

Unperfused mouse eyes were immersion fixed immediately after enucleation ($n = 50$) and within minutes of death by using 4% paraformaldehyde for immunohistochemistry or Ito's fixative[42] for ultramicroscopy. A small incision was made in the cornea or posterior sclera to facilitate fixative entry into the eye. Eyes were shipped overnight in fixative from London to Erlangen.

Immunohistochemistry was performed to label type IV collagen or α-smooth muscle actin (α-SMA) on paraffin sections of three DEX-treated, two sham-treated, and four naïve C57BL/6 mice from a separate colony. Following embedding, 5-μm sagittal sections were cut, deparaffinized in xylol, and washed in PBS. Sections were incubated for 1 hour in blocking buffer (BLOTTO; Santa Cruz Biotechnology; Heidelberg, Germany) at room temperature to prevent nonspecific binding. Sections were incubated overnight at 4°C with primary rabbit monoclonal antibody against α-SMA (Clone EPR5368; Epitomics-Abcam, Burlingame, CA, USA) at a dilution of 1:500 or primary rabbit polyclonal antibody against type IV collagen (AB756P; Chemicon-Millipore, Temecula, CA, USA) at a dilution of 1:100. Primary antibodies were diluted in PBS containing 2% bovine serum albumin (Merck, Darmstadt, Germany) and 0.2% Triton X-100. Sections were then rinsed three times with PBS for 10 minutes each, and incubated for 2 hours with affinity-purified anti-rabbit secondary monoclonal antibody Alexa 488 or 555 (MobiTec, Göttingen, Germany) at a dilution of 1:500. Sections were rinsed in PBS and mounted in Kaiser's glycerin jelly (Merck KGaA, Darmstadt, Germany). Specimens were examined and photographed using a Biorevo BZ-9000 microscope (Keyence; Higashi-Nakajima, Osaka, Japan). Negative controls were treated identically except that the primary antibodies were omitted.

For electron microscopy, 41 eyes (22 DEX-treated and 19 sham-treated controls) were postfixed in OsO_4 and dehydrated. Whole eyes were embedded in Epon resin and 1 μm semithin or ultrathin sections were cut using an ultramicrotome (Ultracut E; Reichert Jung, Vienna, Austria). Semithin sections were stained with toluidine blue, and ultrathin sections were stained with uranyl acetate and lead citrate. Analysis included sagittal sections through the entire anterior-posterior extension of the globe and tangential sections parallel to the plane of the inner wall. To obtain the tangential sections, consecutive semithin sections were taken through the cornea and sclera in a plane parallel to the outer surface of the limbus. Once the lumen of SC was reached, consecutive ultrathin sections were taken and examined until the inner wall of SC, then the JCT and finally the

Investigative Ophthalmology & Visual Science

lamellated TM was reached. Semithin sections were viewed with a Biorevo BZ-9000 microscope (Keyence, Mechelen, Belgium), and ultrathin sections were viewed with an electron microscope (EM 902; Zeiss, Oberkochen, Germany).

Quantitative Measurement of Basement Membrane Material

To quantify the changes in BMM in response to DEX, the fractions of inner wall length exhibiting continuous BMM were measured in seven DEX-treated and five sham-treated control eyes from cohorts 2 and 3. Continuous basement membrane was identified as a thin line of basal lamina-like structure formed by fine fibrillar and granular material underlying the inner wall endothelium of SC as seen at ×12,000 magnification. If fibrillar material was lacking, and only a line of granular material was observed underlying the inner wall endothelium, then this region was not considered to be BMM and was not included in the measurement of basement membrane length (cf. Fig. 4A). The basement membrane length was measured in contiguous sagittal sections (×12,000) spanning the entire anterior-to-posterior length of SC. For this purpose, slot grids coated with Pioloform (Plano, Wetzlar, Germany) were used. Typically, two or three anterior-to-posterior sections (31 sections in total), with 1- to 2-mm separation between sections, could be obtained and were included in the analysis for each eye (one control eye had a single section). The length of each continuous portion of basement membrane was measured and summed to calculate the total basement membrane length for that section, and the total basement membrane length was divided by the total inner wall length for that section. This quotient was averaged over the one to three anterior-to-posterior sections to calculate the percent inner wall length with underlying BMM for each eye. Measurements were performed directly on the microscope using commercial software (analySIS software, ver. 3.1; Olympus Soft Imaging Solutions GmbH, Münster, Germany).

The length of basement membrane underlying the inner wall of SC was also measured in human eyes with long-term corticosteroid treatment and the diagnosis of glaucoma ($n = 7$) archived from a prior study.[23] These were compared against ostensibly normal eyes without corticosteroid treatment ($n = 5$) also taken from the same study.[23] All eyes were from 60- to 80-year-old donors and were immersion fixed after enucleation. Eyes were processed and sectioned for electron microscopy, but because the full anterior-posterior extent of the inner wall was too long to fit within a single section, only regions from the middle portion of the inner wall were used for basement membrane measurements in human eyes. The basement membrane length was measured as described above for mice, and divided by the length of inner wall included within the sections. Sections were included from three to four quadrants per eye.

Statistical Analysis

A repeated-measures Generalized Linear Model (GLM) was used to test the effects of DEX on IOP and body mass (SPSS Advanced Statistics module, version 20; IBM). Within-subject factors were defined to be IOP or body mass, whereas between-subject factors were defined as treatment (DEX or control) and cohort. The GLM model allowed a full factorial design with polynomial contrasts to account for dependence on time (with baseline defined as time 0). Pairwise comparisons were performed using a post hoc Bonferroni test. Because the GLM algorithm ignores data from any individual containing at least one missing data point, we performed the GLM analysis between baseline and week 3 so as to include data from cohort 3 that was missing week 4 IOP data. A total of 21 DEX-treated and 28 sham-treated control mice across all 3 cohorts had complete IOP data between 0 and 3 weeks and were included in the GLM analysis (10 DEX-treated mice dropped out before 3 weeks). There were no outliers in the IOP and body mass data sets.

Statistical tests on outflow facility and basement membrane length were performed using a GLM univariate ANOVA (SPSS), with a full factorial design where the fixed factor was defined as the treatment group and the random factor defined as the cohort. Outliers for the facility analysis were identified based on Dixon's Q-test with a 95% confidence threshold.[43] Based on this criterion, the conventional outflow facility from one DEX-treated mouse was found to be an outlier and excluded from statistical analysis. Linear regression analysis was performed using SPSS, with outliers for the linear regression defined as those points having a Cook's distance larger than unity. Based on this criterion, one data point was excluded from the correlation between outflow facility and basement membrane length. The significance threshold was defined to be 0.05.

Results

Intraocular pressure and *C* Changes in Response to DEX

Systemic DEX-treatment resulted in sustained OHT of 2 to 3 mm Hg in all three cohorts of mice ($P = 2 \times 10^{-10}$, 95% confidence interval: 2.0–3.3 mm Hg, $n = 21$ DEX and 28 control mice excluding drop-outs; Fig. 1A, Supplementary Fig. S2). Intraocular pressure elevation was rapid and typically occurred within 1 week following the onset of DEX delivery, increasing from 15.4 ± 1.9 to 18.6 ± 3.5 mm Hg (mean ± SD; $n = 30$) between baseline (BL) and week 1. Ocular hypertension was sustained throughout the 28-day operational life of the mini-pump, such that at 3 to 4 weeks after surgery, IOP was 18.9 ± 3.0 mm Hg in DEX-treated mice ($n = 21$) versus 14.1 ± 1.8 mm Hg in sham-treated mice ($n = 28$). A histogram of the IOP values measured 3 to 4 weeks after surgery (Supplementary Fig. S3) revealed that some DEX-treated mice have IOP values within the range of the sham-treated controls, but no evidence for a bimodal distribution to suggest a subpopulation of steroid "nonresponders." In contrast, IOP remained near BL levels in sham-treated mice, with the exception of a transient increase of nearly 2 mm Hg between BL and week 1 (15.0 ± 2.9 to 16.7 ± 2.5 mm Hg; $n = 28$).

As measured by perfusion of enucleated eyes, systemic DEX treatment led to a decrease in the perfusion flow rate at each perfusion pressure compared with sham-treated control eyes (Fig. 1B, Supplementary Fig. S3). The slope of the flow versus pressure relationship represents *C* and was 0.018 ± 0.005 μL/min/mm Hg in control mice ($n = 11$) and 0.008 ± 0.001 μL/min/mm Hg in DEX-treated mice ($n = 9$, excluding one outlier), representing a 56% ± 17% reduction in *C* caused by DEX ($P = 1 \times 10^{-5}$; GLM ANOVA; Fig. 1C). The zero pressure intercept of the flow versus pressure relationship, often assumed to represent unconventional outflow,[33,39] was nearly zero in DEX-treated mice (–0.003 ± 0.019 μL/min; $n = 10$), but significantly more negative in sham-treated control mice (–0.024 ± 0.024 μL/min, $n = 11$; $P = 0.005$; Fig. 1C). There was a statistically significant relationship between IOP measured immediately before death and outflow resistance (1/*C*) measured in the same mouse after enucleation ($P = 0.007$, $R^2 = 0.33$, $n = 10$ DEX and 11 control mice; Fig. 1D), suggesting that elevated IOP caused by DEX was partly attributable to reduced *C*. Cohort 1 was excluded from the facility analysis above because perfusion of that cohort was

Investigative Ophthalmology & Visual Science

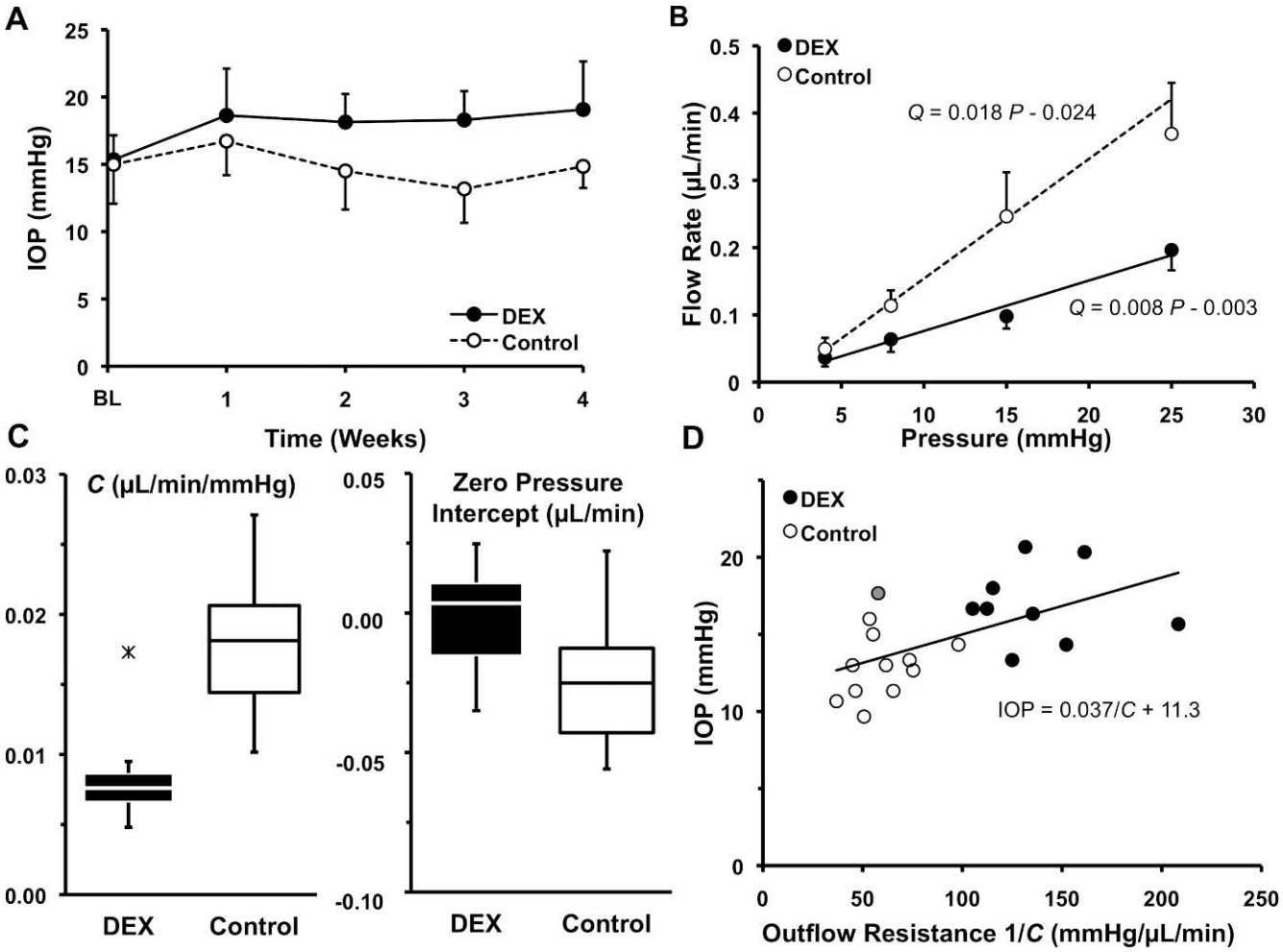

Figure 1. Systemic DEX increases IOP and decreases conventional outflow facility in mice. (**A**) Intraocular pressure as a function of time after surgery for DEX (*filled circles*) and sham-treated control mice (*open circles*) averaged over all three cohorts ($P = 2 \times 10^{-10}$; $N = 31$ DEX-treated and 28 sham-treated control mice at baseline; $n = 21$ DEX and 28 controls at week 3). For cohorts 1 and 2, BL was taken immediately before surgery, whereas for cohort 3, BL was taken 5 to 8 days before surgery. Cohort 3 was terminated after 3 weeks and was not included in the 4-week time point. *Bars* are SD. (**B**) The perfusion flow rate (mean ± SD) as a function of perfusion pressure in enucleated eyes from DEX-treated (*filled circles*; $n = 9$) and sham-treated control mice (*open circles*; $n = 11$). The *trend lines* represent the slope and intercept of the fitted flow rate (Q) versus pressure (P) relationship averaged over all perfusions for each group (excluding one outlier in the DEX-treated group). Data are from cohorts 2 and 3 only, where perfusions were done at physiological temperature and hydration. (**C**) Box and whisker plots for the slope, representing conventional outflow facility (C), and zero pressure intercept of the flow rate versus pressure relationship for DEX-treated and sham-treated control mice. The decrease in C with DEX is statistically significant ($P = 1 \times 10^{-5}$). The zero pressure intercept is often assumed to represent the unconventional outflow rate. *Whiskers* represent the range, *box edges* represent the first and third quartiles, and the *centerline* represents the median, excluding one outlier (*asterisk*). (**D**) Intraocular pressure measured immediately before death plotted as a function of conventional outflow resistance ($1/C$) measured in the same mouse after enucleation for DEX-treated (*filled circles*, $n = 10$) and sham-treated control mice (*open circles*, $n = 11$) from cohorts 2 and 3. The *gray-shaded data point* represents the outlier from the DEX group identified in (**C**). The slope of the line of best fit is statistically significant ($P = 0.007$; $R^2 = 0.33$, including outlier), suggesting that elevated IOP following DEX is due in large part to obstruction of the conventional outflow pathway. Supplementary Figures S2 and S3 show IOP and C data from each cohort separately.

done under different experimental conditions than for cohorts 2 and 3 (see Methods). Repeating the analysis including all three cohorts (including outliers) had little effect on the results, and the facility reduction caused by DEX remained highly significant (50% ± 27%, $n = 15$ DEX and 16 control mice, $P = 4 \times 10^{-5}$; GLM ANOVA), as did the relationship between IOP and $1/C$ ($P = 0.002$, $R^2 = 0.30$, $n = 31$).

Serum DEX Concentration and Body Mass

The serum DEX concentration ($n = 11$ mice from cohort 2) was similar between day 3 and day 10 (105 ± 49 ng/mL lumped mean), but decreased to 47 ± 31 ng/mL by 28 days (Supplementary Fig. S4A). In contrast, the serum DEX concentration in the control group ($n = 8$ mice) remained below the quantitative detection limit (≤10 ng/mL) for all mice at all time points examined (day 3, 10, and 28). In the treated group, there was a large coefficient of variation (CV, ratio of SD to mean) in serum DEX concentration within any given individual over time (CV = 64% ± 40%) and between individuals at any given time point (CV = 61% ± 4%). DEX-treated mice lost more body mass compared with sham-treated mice ($P = 3 \times 10^{-8}$, $n = 21$ DEX and 28 control mice; Supplementary Fig. S4B), despite the DEX-treated mice being put on high-calorie chow. The loss in body mass contributed to a dropout rate reaching 40% by 3 to 4 weeks in DEX-treated mice (Supplementary Fig. S4C).

Investigative Ophthalmology & Visual Science

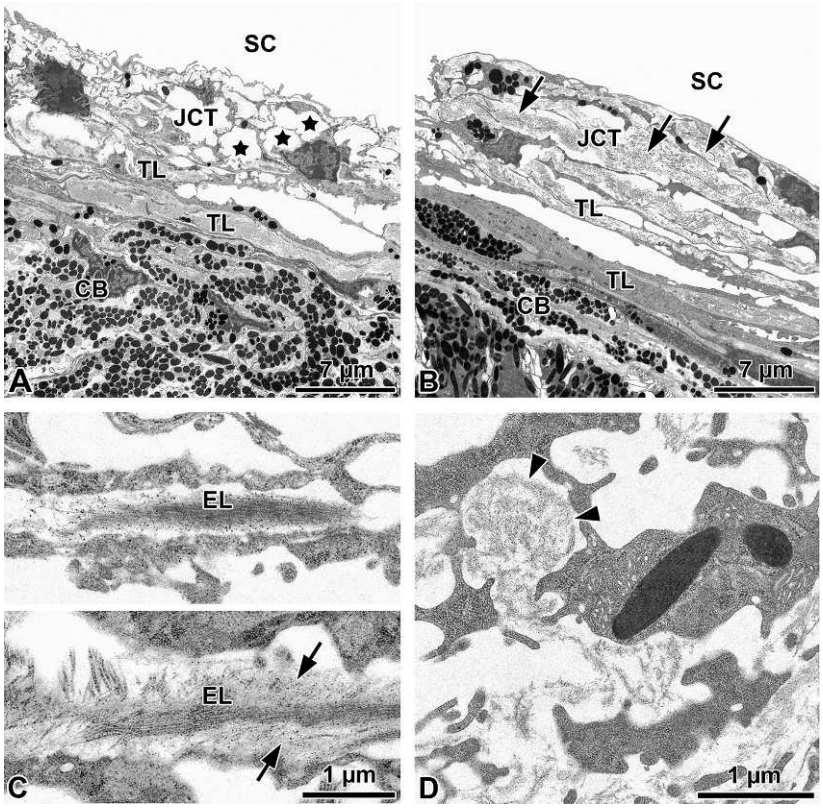

Figure 2. Ultrastructural changes in the JCT of mice treated with or without DEX for 3 to 4 weeks. (**A**) In sham-treated control mice without DEX, optically open spaces (*stars*) were often observed between JCT cells with processes extending in many directions. (**B**) In DEX-treated mice, the JCT was often filled with fine fibrillar material (*arrows*), and the JCT cells appeared elongated. (**C**) The elastic fibers (EL) in the JCT were typically surrounded by a thin coating of fine fibrillar or "sheath" material in control eyes without DEX (*top*) that increased in thickness with DEX (*bottom*, *arrows*). (**D**) Coiled BMM (*arrowheads*) was found within the JCT of DEX-treated mice. CB, ciliary body; TL, trabecular lamellae.

Ultrastructural and Histological Changes in Response to DEX

As seen in sagittal ultrathin sections, DEX treatment led to an accumulation of fine fibrillar material in the TM and between the 3 to 4 layers of cells within the JCT, compared with the optically open spaces in the JCT of sham-treated control mice (Figs. 2A, 2B). In some parts of the circumference of DEX-treated mice, where the increase in fibrils was most prominent, the JCT cells appeared elongated in the anterior-posterior direction as if under tension, compared with the stellate appearance of JCT cells in the sham-treated controls, where JCT cell processes extended in many directions. An increase in fine fibrillar material was also seen surrounding the elastic fibers in the TM in DEX-treated mice (Fig. 2C); such fibers were especially numerous in places where elastic fibers connected to inner wall or to JCT cells. In some parts of the circumference in DEX-treated mice, coiled BMM was present in the TM (Fig. 2D) that showed some similarities to the "fingerprint"-like BMM described in human eyes treated with corticosteroids.[23]

By immunohistochemistry, type IV collagen labeling along the inner wall endothelium of SC appeared more pronounced and continuous in DEX-treated eyes compared with controls (Figs. 3A, 3B). By electron microscopy, there was increased BMM underlying the inner wall endothelium of SC of DEX-treated mice (Figs. 3C, 3D). In oblique sections through the inner wall, the ground substance of the basement membrane appeared more osmiophilic in DEX-treated mice compared with controls (Figs. 3E, 3F), suggesting qualitative changes to the composition of the inner wall basement membrane in response to DEX. As measured in 31 sagittal sections (Fig. 4A), the length of inner wall basement membrane increased from 28.9% ± 13.3% in control mice ($n = 5$) to 75.7% ± 8.3% in DEX-treated mice ($P = 0.0003$, $n = 7$; Fig. 4B). The length of inner wall basement membrane was correlated with decreasing C ($P = 0.001$, $R^2 = 0.74$, $n = 10$, one outlier removed; Fig. 4C) and increasing IOP measured before death ($P = 0.007$, $R^2 = 0.57$, $n = 11$; data not shown).

By immunohistochemistry in DEX-treated eyes, but not in controls, positive α-SMA labeling was observed in cells adjacent to the outer wall endothelium of SC, but not elsewhere in the sclera (Figs. 5A, 5B). Intense α-SMA labeling was also observed in the TM and may have increased in response to DEX. At the ultrastructural level, cells adjacent to the outer wall of DEX-treated mice often contained dense intracellular filaments and were surrounded by an incomplete basement membrane and a matrix containing smaller collagen fibrils and more ground substance compared with the deeper sclera (Figs. 5C, 5D). These data suggest that DEX, or the OHT caused by DEX, induces transformation of scleral fibroblasts into myofibroblasts along the outer wall of SC.

Human Eyes With Long-Term Corticosteroid Treatment

Motivated by the finding that BMM increases in mice treated with DEX, we examined the basement membrane underlying the inner wall of SC in human eyes with long-term corticosteroid treatment and a diagnosis of glaucoma archived

Investigative Ophthalmology & Visual Science

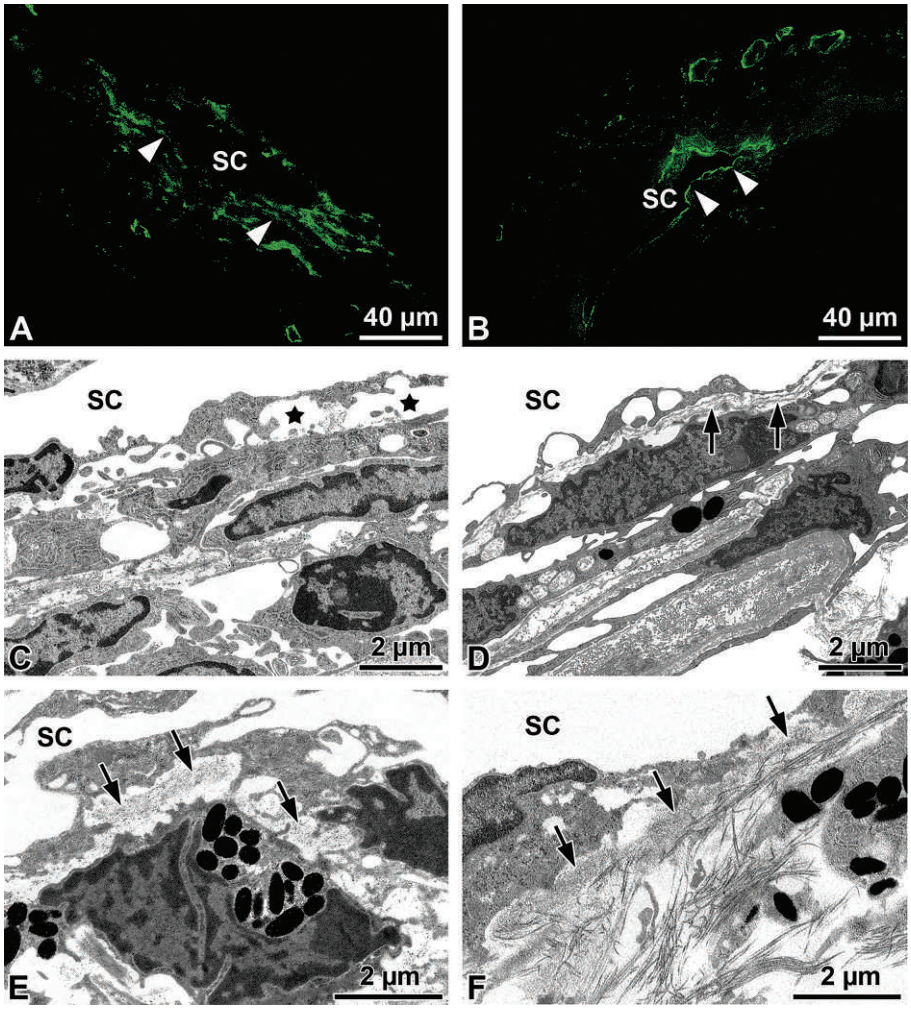

FIGURE 3. The morphology of the basement membrane underlying the inner wall endothelium of SC with or without DEX treatment. (**A**) By immunofluorescence microscopy in sagittal sections, staining type IV collagen (*green*) was present in the TM and along the inner and outer walls of SC (*arrowheads*) in sham-treated control mice, but the distribution tended to be patchy and discontinuous. (**B**) Dexamethasone-treated mice, in contrast, showed a more continuous labeling of type IV collagen along the inner wall of SC (*arrowheads*). *Arrowheads* indicate the inner wall of SC in (**A**) and (**B**). (**C**) By electron microscopy, sham-treated control mice show a patchy and discontinuous basement membrane underlying the inner wall endothelium of SC with frequent open spaces immediately underneath inner wall SC cells (*stars*, *sagittal section*). (**D**) Dexamethasone-treated mice show a more continuous and dense basement membrane (*arrows*) underlying the inner wall of SC (*sagittal section*). (**E**) Oblique sections through the inner wall of SC in sham-treated control mice show that the basement membrane, where present, consists of a loosely arranged net filled with granular material (*arrows*) interspersed between SC cell processes and open spaces. (**F**) Oblique sections through the inner wall of SC in DEX-treated mice reveal a net that is filled with electron-dense BMM (*arrows*), indicating that the inner wall basement membrane is qualitatively different compared with that in sham-treated control mice shown in (**E**).

from a previous study.[23] As observed in DEX-treated mice, SC basement membrane was more continuous in corticosteroid-treated human eyes, appearing as a dense band of ECM approximately 0.1-µm thick immediately underlying the SC cells (Fig. 6). Quantifying the length of SC basement membrane revealed a 5- to 6-fold increase between human eyes without corticosteroids (9.9% ± 4.1%) and age-matched human eyes with SIG (55.5% ± 22.6%; $P = 0.001$, Student's *t*-test; Fig. 6C). These data suggest that ultrastructural changes in the inner wall basement membrane may contribute to outflow obstruction in human SIG.

DISCUSSION

This project investigated DEX-induced OHT in mice. Within 1 week of systemic DEX, IOP became elevated by 2 to 3 mm Hg, and IOP elevation was sustained throughout the entire 3- to 4-week duration of the study. Conventional outflow facility was reduced by 52%, and there was a correlation between elevated IOP and decreased *C*. These data suggest that increased aqueous humor outflow resistance contributed to DEX-induced OHT in mice, as in other species. In mice, our results were consistent with previous studies of corticosteroid-induced OHT, including Whitlock et al.[18] who first described IOP elevation by systemic DEX, Zode et al.[21] who reported IOP elevation in response to topical ocular DEX, and Kumar et al.[19,20] who reported decreased *C* by subconjunctival triamcinolone acetonide (but without IOP elevation). Ultrastructural analyses revealed that DEX increased ECM in the JCT, including fine fibrillar material and BMM immediately underlying the inner wall endothelium of SC. Because the bulk of outflow resistance is likely generated near the JCT and inner wall, at least in primates,[44,45] accumulation of ECM in these tissues could have contributed to conventional outflow obstruction following DEX. Indeed, our studies revealed a correlation

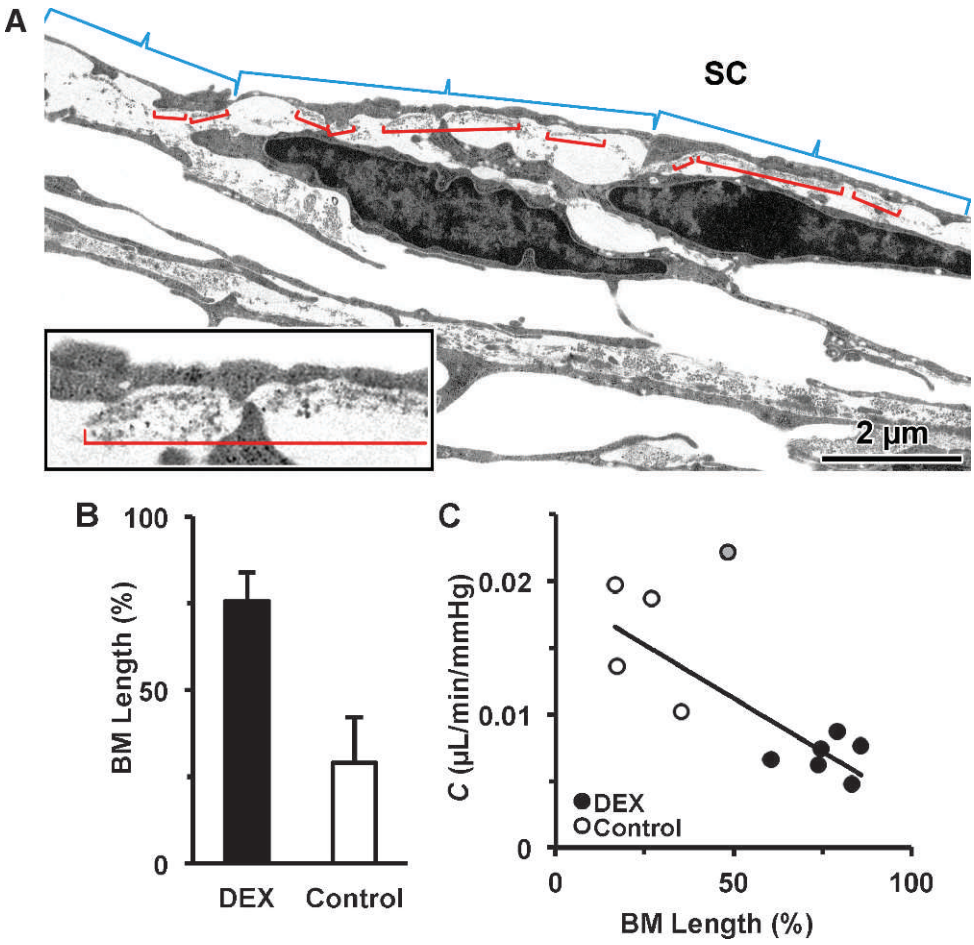

FIGURE 4. The basement membrane underlying the inner wall endothelium of SC becomes more continuous following systemic DEX treatment. (**A**) Continuous sections of the inner wall basement membrane (*red brackets*) were identified based on the presence of a thin basal lamina–like structure immediately underlying the inner wall endothelium. The length of basement membrane was then divided by the total length of the inner wall endothelium (*blue brackets*) to calculate the basement membrane length expressed as a percentage of the total inner wall length. (**B**) The basement membrane (BM) length in DEX-treated ($n = 7$ eyes) and sham-treated control mice ($n = 5$) measured along the entire anterior-posterior length of SC in three independent sagittal sections per eye. The increase in BM length with DEX is statistically significant ($P = 0.0003$). *Bars* are SD. (**C**) Conventional outflow facility (C) plotted versus BM length measured in contralateral eyes of the same mouse from DEX-treated (*black circles*) and sham-treated control mice (*white circles*). The relationship was statistically significant ($P = 0.001$, $R^2 = 0.74$). The data point indicated by the *gray circle* was found to be an outlier (Cook's distance = 1.3) and was excluded from the regression analysis, but the relationship remained significant even if the outlier was included ($P = 0.009$, $R^2 = 0.55$). Data in (**B**) and (**C**) are from cohorts 2 and 3 only.

between C and length of basement membrane underlying the inner wall of SC.

The ultrastructural changes in the TM of DEX-treated mice closely resembled the changes previously described in corticosteroid-treated human eyes. Namely, in DEX-treated mice there was an accumulation of fine fibrillar material and coiled BMM in the JCT that shows some similarities to the "fingerprint"-like material described in living human eyes treated with corticosteroids[23,27] and in organ-cultured human eyes perfused with DEX.[28] As in corticosteroid-treated human eyes,[23] there was a pronounced increase in myofibroblasts along the outer wall of SC in DEX-treated mice, and the fibrillar ECM surrounding these myofibroblasts differed from the thicker collagen fibers in the deeper sclera. Although corticosteroid-induced alterations to the inner wall basement membrane have not been described extensively, our findings in mice motivated a reexamination of archived human SIG specimens[23] and revealed a similar increase in the basement membrane length along SC compared with age-matched human specimens that did not receive corticosteroids. These data demonstrate that DEX-treated mice mimic several hallmarks of SIG in humans, including IOP elevation, conventional outflow obstruction, ECM accumulation, and myofibroblast transformation within the outflow pathway. Therefore, DEX-treated mice may provide an excellent model system for investigating the pathogenesis of SIG as occurs in humans.

Following DEX, there was increased thickness of the fibrillar material surrounding elastic fibers in the JCT that partially resembled the "sheath-derived" plaques described in human TM.[46] Sheath-derived plaques become thicker with age and with glaucoma,[47] and sheath-derived–like plaque material has been described in the JCT of bovine eyes treated with corticosteroids.[9] Although the hydrodynamic consequences of sheath-derived plaques remain unclear,[48,49] it is generally believed that sheath-derived plaques play a role in TM dysfunction in POAG.[50] In DEX-treated mice, however, the fine fibrillar material surrounding the elastic fibers did not exhibit the typical 50-nm banding periodicity observed for sheath-derived plaques in human TM,[51] and therefore mice did not form "true" sheath-derived plaques in response to DEX. The details of sheath-derived plaque development are largely unknown, but the initial thickening of the fibrillar sheath

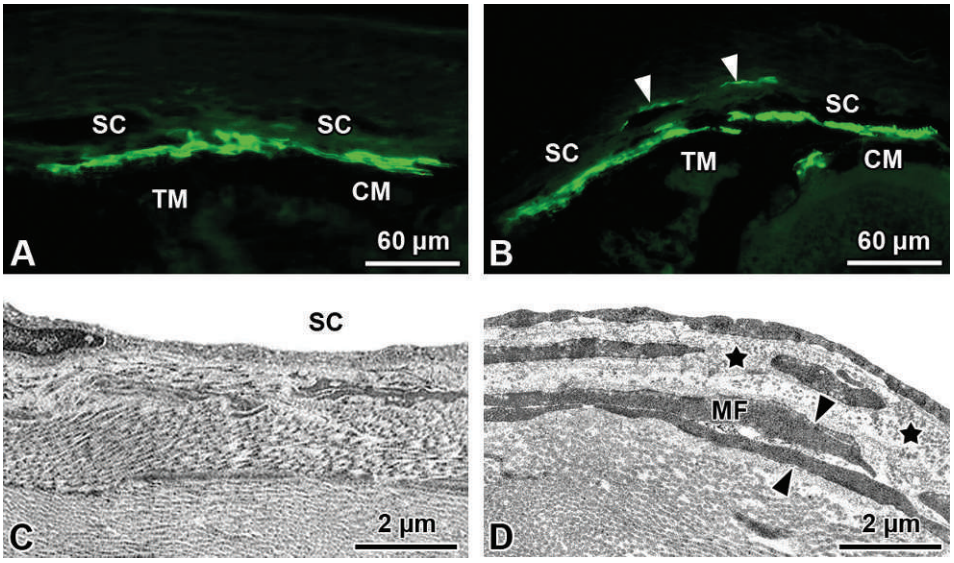

Figure 5. Myofibroblasts along the outer wall of SC in mice treated with systemic DEX. (**A**) In sham-treated control mice, there is dense labeling of α-SMA in the ciliary muscle (CM), and many cells within the TM express α-SMA. (**B**) Following DEX, there is an increase in α-SMA labeling along the outer wall of SC (*arrowheads*) and possibly in the TM. (**C**) In sham-treated control mice, as seen by transmission electron microscopy (TEM), the outer wall of SC contains few cells between the endothelium and the deeper sclera. (**D**) In DEX-treated mice, as seen by TEM, the outer wall of SC reveals the presence of myofibroblasts (MF), indicated by dense cytoplasmic filaments and incomplete basement membranes (*arrowheads*). The ECM surrounding the MF is loosely arranged with smaller fibers (*stars*) relative to the deeper sclera.

suggests that DEX-treated mice may provide a promising model to investigate the early-stage development of sheath-derived plaques.

Ultrastructural analysis revealed a more pronounced and continuous basement membrane underlying the inner wall endothelium of SC following DEX, and increased length of inner wall basement membrane was correlated with decreased *C*. These data suggested that accumulation of BMM along the inner wall of SC might contribute to outflow obstruction in response to DEX. However, the resistance generated by the inner wall basement membrane on its own could not account for more than a small fraction of the total outflow resistance on account of its many discontinuities[52] that are present even within DEX-treated mice. It is tempting to speculate, however, that the inner wall basement membrane may channel or "funnel" outflow through these discontinuities so as to

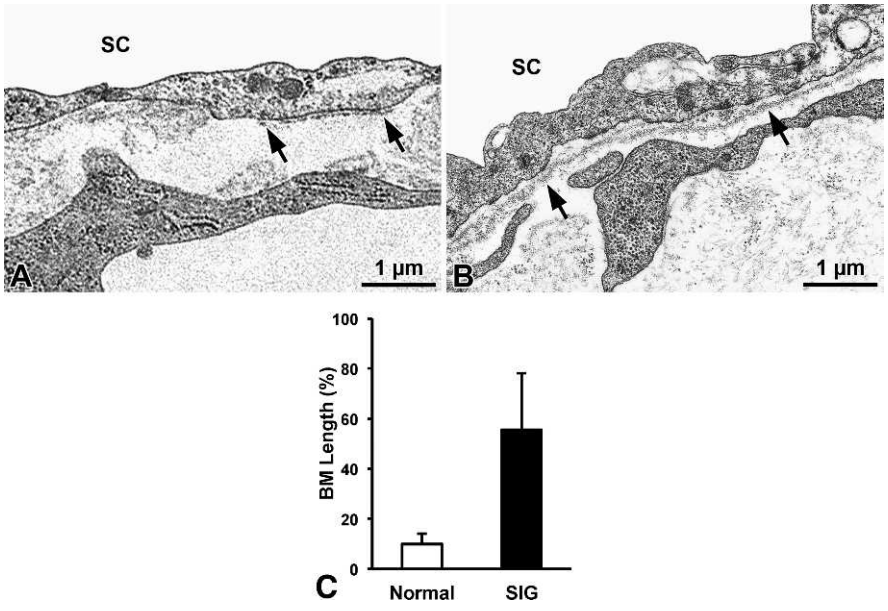

Figure 6. Ultrastructure of the basement membrane underlying the inner wall of SC in human eyes treated with or without corticosteroids archived from a previous study.[23] (**A**) Electron micrograph of SC inner wall showing a small region of basement membrane (*arrows*) typical for normal human eyes without steroid treatment (65-year-old female). The amorphous material on the left side was not considered to be basement membrane. (**B**) The basement membrane (*arrows*) underlying the inner wall endothelium of SC appears as a continuous dark band of ECM in a human eye treated with corticosteroids (63-year-old female). (**C**) The length of the inner wall basement membrane (BM) is greater in human eyes diagnosed with SIG ($n = 7$) compared with normal human eyes without corticosteroid treatment ($n = 5$; $P = 0.001$; Student's *t*-test).

modulate or augment resistance generation in the JCT as previously proposed[53] as a modification to the conventional funneling hypothesis.[54] DEX, by causing the basement membrane to become more continuous, may have increased the effective outflow resistance generated in the JCT by modulating the funneling effect. Consistent with this idea, DEX is known to stimulate basement membrane synthesis[55] and turnover[56–58] that may have contributed to a progressive accumulation of ECM in DEX-treated mice. Alternatively, DEX reduces the permeability of endothelial barriers and tightens intercellular junctions in SC cells,[59,60] and changes to the inner wall basement membrane may in fact be secondary to changes in the properties of SC cells themselves. Future studies examining the ultrastructural changes to SC cells and basement membrane over time following DEX may provide insight into the mechanisms of outflow resistance elevation in corticosteroid-induced OHT.

Previous studies of corticosteroid-induced OHT typically describe a subpopulation of "nonresponders" who fail to exhibit IOP elevation despite prolonged steroid treatment. In mice of mixed genetic background, Whitlock et al.[18] reported that approximately one-third of those receiving DEX via subcutaneous mini-pump failed to exhibit an IOP elevation exceeding 2 SDs from the baseline mean. Zode et al.,[21] in contrast, reported IOP elevation in 90% or more of inbred mice receiving topical ocular DEX. Similarly, our current study using inbred mice showed no clear evidence for a subpopulation of steroid nonresponders, despite some DEX-treated mice having IOP values that fell within the range of the control population. These data suggest that steroid responsiveness may be associated with genetic background in mice. However, without clear evidence for bimodality in IOP histogram, it is difficult to determine whether the DEX-treated mice with low IOPs are true "nonresponders" or simply those individuals that fall near the low end of the IOP distribution where some overlap with the baseline distribution may be expected.[18]

A disadvantage of the implantable mini-pumps is the inability to regulate or target DEX delivery. For instance, the serum DEX concentration varies by nearly 60% between individuals despite identical mini-pump loading conditions, and it is uncertain how variability in serum DEX levels may influence the IOP response or the IOP distribution in the treated population. Furthermore, with systemic DEX treatment, mice experience adverse effects, including weight loss, and it would therefore be desirable to reduce the DEX dosage after implantation so as to minimize distress and dropout. These limitations may be overcome by using alternative methods that provide more consistent, tunable, or targeted DEX delivery to achieve sufficient IOP elevation with minimal systemic effects.

Relationship Between IOP and *C*

It is useful to examine whether the reduction in C in response to DEX was sufficient to explain the elevation in IOP. According to Goldmann's equation, IOP may be written in terms of conventional outflow resistance ($1/C$) as follows:

$$\mathrm{IOP} = \frac{1}{C}(F_{in} - F_u) + \mathrm{EVP} \qquad (2)$$

where F_{in} is the aqueous production rate, F_u is the unconventional outflow rate, and EVP is episcleral venous pressure. Assuming that the conventional outflow rate ($F_c = F_{in} - F_u$) and EVP remain constant, then Equation 2 predicts a linear relationship between IOP and $1/C$ across any arbitrary population of mice (or any species for that matter). As shown in Figure 1D, despite DEX-treated mice having larger values of IOP and $1/C$, the entire population was well described by a linear relationship between IOP and $1/C$, consistent with Equation 2. Deviations from the line of best fit were likely attributable to measurement errors in IOP or $1/C$ or to fluctuations in EVP or F_c between individuals. Regardless, the statistical significance of the correlation suggests that elevated IOP following DEX is due to an increase in $1/C$ and an effective "translation" of the population to the right (to higher values of $1/C$) along the regression shown in Figure 1D. According to Equation 2, the slope of the line of best fit between IOP and $1/C$ estimates F_c, whereas the intercept (at $1/C = 0$) estimates EVP,[39] yielding $F_c = 0.037 \pm 0.012$ μL/min and EVP = 11.3 ± 1.3 mm Hg (mean ± SEM). These predictions are indirect and differ from direct measurements of F_c (0.062 μL/min) and EVP (6.5 mm Hg) measured in the same strain of mice.[61]

Alternatively, one may examine the population statistics to determine whether the mean decrease in C is sufficient to explain the mean increase in IOP. Because Goldmann's equation is strictly true for individual eyes and not populations of eyes, we may take the expected value of Equation 2, neglecting any covariance between F_c and $1/C$ to obtain[39]:

$$\overline{\mathrm{IOP}} = \overline{F_c}\,\overline{R} + \overline{\mathrm{EVP}} \qquad (3)$$

where overbars indicate population averages and $\overline{R}$ represents the average value of $1/C$. Assuming that $\overline{F_c}$ and $\overline{\mathrm{EVP}}$ are constants and unaffected by DEX, then we may express Equation 3 as

$$\frac{\overline{R_d}}{\overline{R_s}} = \frac{\overline{\mathrm{IOP}_d} - \overline{\mathrm{EVP}}}{\overline{\mathrm{IOP}_s} - \overline{\mathrm{EVP}}} \qquad (4)$$

where the subscripts "d" and "s" refer to DEX-treated and sham-treated controls, respectively. Limiting the analysis to only those data from cohorts 2 and 3 where C and IOP were measured in the same individuals, yields $\overline{\mathrm{IOP}_d} = 17.0 \pm 2.3$ mm Hg (mean ± SD) and $\overline{R_d} = 130 \pm 39$ mm Hg/μL/min for DEX-treated mice ($n = 10$), and $\overline{\mathrm{IOP}_s} = 12.8 \pm 1.9$ mm Hg and $\overline{R_s} = 60 \pm 17$ mm Hg/μL/min for sham-treated control mice ($n = 11$). The right-hand side of Equation 4 depends on the value of $\overline{\mathrm{EVP}}$, which is unknown, but if $\overline{\mathrm{EVP}} = 9.2$ mm Hg, then the relative change in conventional outflow resistance can fully account for the change in IOP with DEX. If $\overline{\mathrm{EVP}}$ is less than 9.2 mm Hg, which seems possible based on the single study that directly measured $\overline{\mathrm{EVP}}$ to be 6.5 ± 0.3 mm Hg in C57BL/6 mice,[61] then the right-hand side of Equation 4 becomes smaller than the left-hand side, meaning that the change in outflow resistance with DEX is larger than necessary to fully account for the IOP elevation. This conclusion holds even if we allow $\overline{\mathrm{EVP}}$ to increase with DEX (motivated by the observation that DEX increases systolic blood pressure[18]) and let $\overline{\mathrm{EVP}} = 6.5$ mm Hg in the sham-treated control mice. This population-based analysis suggests that within the limitations of our measurement accuracy and assumptions (i.e., constant $\overline{F_c}$), the increase in conventional outflow resistance is sufficient to explain the majority, if not all, of the elevation in IOP following systemic DEX in mice.

In summary, this project examined the mechanism for DEX-induced OHT in mice, showing that IOP elevation can be largely attributed to decreased conventional outflow facility. Obstruction of the conventional outflow pathway appears to be related to accumulation of fine fibrillar ECM in the JCT, increased thickness of sheath material surrounding elastic fibers in the TM, and/or increased length of the basement membrane underlying the inner wall endothelium of SC. Myofibroblasts in the conventional outflow pathway also are present following DEX. These data demonstrate that systemic DEX in mice causes phenotypic changes in the conventional

outflow pathway that mimic the hallmarks of SIG in humans, providing an animal model to study the pathogenesis of TM dysfunction and OHT related to steroid glaucoma.

Acknowledgments

Supported by an unrestricted research gift from Allergan, Inc. Additional support provided by National Glaucoma Research, a Program of the BrightFocus Foundation (formerly as the American Health Assistance Foundation), the National Eye Institute Grant EY022359, and the Dr. Valentin Aplas-Stiftung Foundation.

Disclosure: **D.R. Overby**, Allergan (F); **J. Bertrand**, None; **O.-Y. Tektas**, None; **A. Boussommier-Calleja**, None; **M. Schicht**, None; **C.R. Ethier**, None; **D.F. Woodward**, Allergan (E); **W.D. Stamer**, None; **E. Lütjen-Drecoll**, Allergan (F)

References

1. Goldmann H. Cortisone glaucoma. *Arch Ophthalmol*. 1962; 68:621–626.
2. Bernstein HN, Schwartz B. Effects of long-term systemic steroids on ocular pressure and tonographic values. *Arch Ophthalmol*. 1962;68:742–753.
3. Armaly MF. Effect of corticosteroids on intraocular pressure and fluid dynamics. *Arch Ophthalmol*. 1963;70:482–491.
4. Armaly MF. Statistical attributes of the steroid hypertensive response in the clinically normal eye. I. the demonstration of three levels of response. *Invest Ophthalmol*. 1965;4:187–197.
5. Becker B. Intraocular pressure response to topical corticosteroids. *Invest Ophthalmol*. 1965;4:198–205.
6. Becker B, Hahn KA. Topical corticosteroids and heredity in primary open-angle glaucoma. *Am J Ophthalmol*. 1964;57: 543–551.
7. Clark AF, Wordinger RJ. The role of steroids in outflow resistance. *Exp Eye Res*. 2009;88:752–759.
8. Gerometta R, Podos SM, Candia OA, et al. Steroid-induced ocular hypertension in normal cattle. *Arch Ophthalmol*. 2004; 122:1492–1497.
9. Tektas O-Y, Hammer CM, Danias J, et al. Morphologic changes in the outflow pathways of bovine eyes treated with corticosteroids. *Invest Ophthalmol Vis Sci*. 2010;51:4060–4066.
10. Mao W, Tovar-Vidales T, Yorio T, Wordinger RJ, Clark AF. Perfusion-cultured bovine anterior segments as an ex vivo model for studying glucocorticoid-induced ocular hypertension and glaucoma. *Invest Ophthalmol Vis Sci*. 2011;52:8068–8075.
11. Zhan GL, Miranda OC, Bito LZ. Steroid glaucoma: corticosteroid-induced ocular hypertension in cats. *Exp Eye Res*. 1992; 54:211–218.
12. Bhattacherjee P, Paterson CA, Spellman JM, Graff G, Yanni JM. Pharmacological validation of a feline model of steroid-induced ocular hypertension. *Arch Ophthalmol*. 1999;117: 361–364.
13. Ticho U, Lahav M, Berkowitz S, Yoffe P. Ocular changes in rabbits with corticosteroid-induced ocular hypertension. *Br J Ophthalmol*. 1979;63:646–650.
14. Candia OA, Gerometta R, Millar JC, Podos SM. Suppression of corticosteroid-induced ocular hypertension in sheep by anecortave. *Arch Ophthalmol*. 2010;128:338–343.
15. Gerometta R, Spiga M-G, Borrás T, Candia OA. Treatment of sheep steroid–induced ocular hypertension with a glucocorticoid-inducible MMP1 gene therapy virus. *Invest Ophthalmol Vis Sci*. 2010;51:3042–3048.
16. Gerometta R, Podos SM, Danias J, Candia OA. Steroid-induced ocular hypertension in normal sheep. *Invest Ophthalmol Vis Sci*. 2008;50:669–673.
17. Miyara N, Shinzato M, Yamashiro Y, Iwamatsu A, Kariya K-I, Sawaguchi S. Proteomic analysis of rat retina in a steroid-induced ocular hypertension model: potential vulnerability to oxidative stress. *Jpn J Ophthalmol*. 2008;52:84–90.
18. Whitlock NA, McKnight B, Corcoran KN, Rodriguez LA, Rice DS. Increased intraocular pressure in mice treated with dexamethasone. *Invest Ophthalmol Vis Sci*. 2010;51:6496–6503.
19. Kumar S, Shah S, Tang HM, Smith M, Borrás T, Danias J. Tissue plasminogen activator in trabecular meshwork attenuates steroid induced outflow resistance in mice. *PLoS One*. 2013; 8:e72447.
20. Kumar S, Shah S, Deutsch ER, Tang HM, Danias J. Triamcinolone acetonide decreases outflow facility in C57BL/6 mouse eyes. *Invest Ophthalmol Vis Sci*. 2013;54:1280–1287.
21. Zode GS, Sharma AB, Lin X, et al. Ocular-specific ER stress reduction rescues glaucoma in murine glucocorticoid-induced glaucoma. *J Clin Invest*. 2014;124:1956–1965.
22. Fingert JH, Clark AF, Craig JE, et al. Evaluation of the myocilin (MYOC) glaucoma gene in monkey and human steroid-induced ocular hypertension. *Invest Ophthalmol Vis Sci*. 2001;42:145–152.
23. Johnson D, Gottanka J, Flügel C, Hoffmann F, Futa R, Lütjen-Drecoll E. Ultrastructural changes in the trabecular meshwork of human eyes treated with corticosteroids. *Arch Ophthalmol*. 1997;115:375–383.
24. Clark AF, Steely HT, Dickerson JE, et al. Glucocorticoid induction of the glaucoma gene MYOC in human and monkey trabecular meshwork cells and tissues. *Invest Ophthalmol Vis Sci*. 2001;42:1769–1780.
25. Johnson DH, Knepper PA. Microscale analysis of the glycosaminoglycans of human trabecular meshwork: a study in perfusion cultured eyes. *J Glaucoma*. 1994;3:58–69.
26. Johnson DH, Bradley JM, Acott TS. The effect of dexamethasone on glycosaminoglycans of human trabecular meshwork in perfusion organ culture. *Invest Ophthalmol Vis Sci*. 1990; 31:2568–2571.
27. Rohen JW, Linnér E, Witmer R. Electron microscopic studies on the trabecular meshwork in two cases of corticosteroid-glaucoma. *Exp Eye Res*. 1973;17:19–31.
28. Clark AF, Wilson K, De Kater AW, Allingham RR, McCartney MD. Dexamethasone-induced ocular hypertension in perfusion-cultured human eyes. *Invest Ophthalmol Vis Sci*. 1995; 36:478–489.
29. Smith RS, John SWM, Nishina PM, Sundberg JP. *Systematic Evaluation of the Mouse Eye*. Boca Raton, FL: CRC Press; 2001.
30. Overby DR, Bertrand J, Schicht M, Paulsen F, Stamer WD, Lütjen-Drecoll E. The structure of the trabecular meshwork, its connections to the ciliary muscle and the effect of pilocarpine on outflow facility in mice. *Invest Ophthalmol Vis Sci*. 2014; 55:3727–3736.
31. Savinova OV, Sugiyama F, Martin JE, et al. Intraocular pressure in genetically distinct mice: an update and strain survey. *BMC Genet*. 2001;2:12.
32. Aihara M, Lindsey JD, Weinreb RN. Aqueous humor dynamics in mice. *Invest Ophthalmol Vis Sci*. 2003;44:5168–5173.
33. Lei Y, Overby DR, Boussommier-Calleja A, Stamer WD, Ethier CR. Outflow physiology of the mouse eye: pressure dependence and washout. *Invest Ophthalmol Vis Sci*. 2011;52: 1865–1871.
34. Boussommier-Calleja A, Bertrand J, Woodward DF, Ethier CR, Stamer WD, Overby DR. Pharmacologic manipulation of conventional outflow facility in ex vivo mouse eyes. *Invest Ophthalmol Vis Sci*. 2012;53:5838–5845.
35. Li G, Farsiu S, Chiu SJ, et al. Pilocarpine-induced dilation of Schlemm's canal and prevention of lumen collapse at elevated

intraocular pressures in living mice visualized by OCT. *Invest Ophthalmol Vis Sci*. 2014;55:3737–3746.

36. Wang WH, Millar JC, Pang I-H, Wax MB, Clark AF. Noninvasive measurement of rodent intraocular pressure with a rebound tonometer. *Invest Ophthalmol Vis Sci*. 2005;46:4617–4621.
37. Johnson TV, Fan S, Toris CB. Rebound tonometry in conscious, conditioned mice avoids the acute and profound effects of anesthesia on intraocular pressure. *J Ocul Pharmacol Ther*. 2008;24:175–185.
38. Camras LJ, Sufficool KE, Camras CB, Fan S, Liu H, Toris CB. Duration of anesthesia affects intraocular pressure, but not outflow facility in mice. *Curr Eye Res*. 2010;35:819–827.
39. Boussommier-Calleja A, Overby DR. The influence of genetic background on conventional outflow facility in mice. *Invest Ophthalmol Vis Sci*. 2013;54:8251–8258.
40. Stamer WD, Lei Y, Boussommier-Calleja A, Overby DR, Ethier CR. eNOS, a pressure-dependent regulator of intraocular pressure. *Invest Ophthalmol Vis Sci*. 2011;52:9438–9444.
41. Overby D, Gong H, Qiu G, Freddo TF, Johnson M. The mechanism of increasing outflow facility during washout in the bovine eye. *Invest Ophthalmol Vis Sci*. 2002;43:3455–3464.
42. Ito S, Karnovsky MJ. Formaldehyde-glutaraldehyde fixatives containing trinitro compounds. *J Cell Biol*. 1968;39:168A–169A.
43. Dean RB, Dixon WJ. Simplified statistics for small numbers of observations. *Anal Chem*. 1951;23:636–638.
44. Lütjen-Drecoll E. Structural factors influencing outflow facility and its changeability under drugs. A study in *Macaca arctoides*. *Invest Ophthalmol*. 1973;12:280–294.
45. Mäepea O, Bill A. Pressures in the juxtacanalicular tissue and Schlemm's canal in monkeys. *Exp Eye Res*. 1992;54:879–883.
46. Rohen JW, Witmer R. Electron microscopic studies on the trabecular meshwork in glaucoma simplex. *Albrecht Von Graefes Arch Klin Exp Ophthalmol*. 1972;183:251–266.
47. Lütjen-Drecoll E, Shimizu T, Rohrbach M, Rohen JW. Quantitative analysis of "plaque material" in the inner and outer wall of Schlemm's canal in normal and glaucomatous eyes. *Exp Eye Res*. 1986;42:443–455.
48. Alvarado JA, Yun AJ, Murphy CG. Juxtacanalicular tissue in primary open angle glaucoma and in nonglaucomatous normals. *Arch Ophthalmol*. 1986;104:1517–1528.
49. Murphy CG, Johnson M, Alvarado JA. Juxtacanalicular tissue in pigmentary and primary open angle glaucoma. The hydrodynamic role of pigment and other constituents. *Arch Ophthalmol*. 1992;110:1779–1785.
50. Tektas O-Y, Lütjen-Drecoll E. Structural changes of the trabecular meshwork in different kinds of glaucoma. *Exp Eye Res*. 2009;88:769–775.
51. Lutjen-Drecoll E, Futa R, Rohen JW. Ultrahistochemical studies on tangential sections of the trabecular meshwork in normal and glaucomatous eyes. *Invest Ophthalmol Vis Sci*. 1981;21:563–573.
52. Johnson M. What controls aqueous humour outflow resistance? *Exp Eye Res*. 2006;82:545–557.
53. Overby DR, Stamer WD, Johnson M. The changing paradigm of outflow resistance generation: Towards synergistic models of the JCT and inner wall endothelium. *Exp Eye Res*. 2009;88:656–670.
54. Johnson M, Shapiro A, Ethier CR, Kamm RD. Modulation of outflow resistance by the pores of the inner wall endothelium. *Invest Ophthalmol Vis Sci*. 1992;33:1670–1675.
55. Dickerson JE, Steely HT, English-Wright SL, Clark AF. The effect of dexamethasone on integrin and laminin expression in cultured human trabecular meshwork cells. *Exp Eye Res*. 1998;66:731–738.
56. Snyder RW, Stamer WD, Kramer TR, Seftor RE. Corticosteroid treatment and trabecular meshwork proteases in cell and organ culture supernatants. *Exp Eye Res*. 1993;57:461–468.
57. Samples JR, Alexander JP, Acott TS. Regulation of the levels of human trabecular matrix metalloproteinases and inhibitor by interleukin-1 and dexamethasone. *Invest Ophthalmol Vis Sci*. 1993;34:3386–3395.
58. Flügel-Koch C, Ohlmann A, Fuchshofer R, Welge-Lüssen U, Tamm ER. Thrombospondin-1 in the trabecular meshwork: localization in normal and glaucomatous eyes, and induction by TGF-beta1 and dexamethasone in vitro. *Exp Eye Res*. 2004;79:649–663.
59. Underwood JL, Murphy CG, Chen J, et al. Glucocorticoids regulate transendothelial fluid flow resistance and formation of intercellular junctions. *Am J Physiol*. 1999;277:C330–C342.
60. Fujimoto T, Inoue T, Kameda T, et al. Involvement of rhoA/rho-associated kinase signal transduction pathway in dexamethasone-induced alterations in aqueous outflow. *Invest Ophthalmol Vis Sci*. 2012;53:7097–7108.
61. Lee YS, Tresguerres M, Hess K, et al. Regulation of anterior chamber drainage by bicarbonate-sensitive soluble adenylyl cyclase in the ciliary body. *J Biol Chem*. 2011;286:41353–41358.

Investigative Ophthalmology & Visual Science